Photoexcitation of astrophysically important states in ^{26}Mg. II. Ground-state-transition partial widths

R. J. deBoer,* M. Wiescher, and J. Görres
Joint Institute for Nuclear Astrophysics, Department of Physics, University of Notre Dame, Notre Dame, Indiana 46556, USA

R. Longland and C. Iliadis
Department of Physics and Astronomy, University of North Carolina at Chapel Hill, Chapel Hill, North Carolina 27599, USA and Triangle Universities Nuclear Laboratory, Durham, North Carolina 27708, USA

G. Rusev and A. P. Tonchev
Triangle Universities Nuclear Laboratory, Durham, North Carolina 27708, USA and Department of Physics, Duke University, Durham, North Carolina 27708, USA
(Received 28 June 2010; published 9 August 2010)

The level structure of ^{26}Mg near the neutron-separation energy, which is of interest for s-process nucleosynthesis, was studied at the High Intensity Gamma-Ray Source of the Triangle Universities Nuclear Laboratory using the method of nuclear resonance fluorescence. A nearly monoenergetic and linearly polarized γ-ray beam was used to scan the excitation energy range from 10.5 to 11.7 MeV. For the five states observed, the total widths and partial widths are determined. Precise measurement of these widths is necessary for the prediction of neutron production for the s-process.

DOI: 10.1103/PhysRevC.82.025802 PACS number(s): 26.20.Kn, 23.20.En, 23.20.Js, 27.30.+t

I. INTRODUCTION

The s-process is the mechanism for the formation of about half of the heavy nuclides up to lead [1]. We can observe these elements in their natural abundances in stellar spectra or in meteorite fragments. The s-process proceeds by neutron capture onto stable light elements which subsequently β-decay back toward stability. It was proposed [2] that the ^{22}Ne$(\alpha,n)^{25}$Mg reaction could be a suitable mechanism for neutron production. In stellar environments, ^{22}Ne can be produced by the reaction chain ^{14}N$(\alpha,\gamma)^{18}$F$(\beta^+)^{18}$O$(\alpha,\gamma)^{22}$Ne where ^{14}N is one of the main products of the CNO cycle. Using the temperature and density requirements necessary for α capture onto ^{22}Ne, two astrophysical sites have been proposed for the s-process. Light s-process elements ($\sim 50 > A > \sim 100$) are thought to be created in massive stars ($M > \sim 10\ M_\odot$) during their core helium burning phase [3]. This has been called the "weak component". The other likely site is the thermally pulsing stage of asymptotic giant branch stars [4]. This "main component" produces the heavier s-process isotopes ($\sim 100 > A > \sim 200$). While ^{13}C$(\alpha,n)^{16}$O is considered to be the chief source of neutrons in the main s-process, ^{22}Ne$(\alpha,n)^{25}$Mg may also have a dominant role.

As a main source of neutrons for the s-process the uncertainty in the ^{22}Ne$(\alpha,n)^{25}$Mg reaction rate as well as the competing reaction ^{22}Ne$(\alpha,\gamma)^{26}$Mg have a significant effect on heavy-element production [5–7]. The critical-temperature region of this reaction in the s-process sites described above is approximately 0.3 GK. This corresponds to a Gamow peak range of 300 keV $< E_{\text{c.m.}} <$ 900 keV or a ^{26}Mg excitation energy of 10.9 MeV $< E_x <$ 11.5 MeV. Above the neutron-separation energy ($S_n = 11093.07(3)$ keV [8]) both the (α,n) and (α,γ) reaction channels compete for the dominant exit channel. The level density at these excitation energies is high with a mean level spacing of $\sim$9 keV. The number of levels available for the ^{22}Ne + α reactions is somewhat reduced because only states with natural parity can contribute. The partial widths are of critical importance since they determine which of the two competing reactions will dominate at a given temperature. Therefore, a detailed knowledge of the level parameters in the Gamow peak region is necessary for an accurate estimation of the rates.

Several experiments have been performed making direct measurements of the ^{22}Ne$(\alpha,n)^{25}$Mg [9–14] and ^{22}Ne$(\alpha,\gamma)^{26}$Mg [13,15] reactions. These measurements have been unable to access the astrophysical energy region because of the relatively high α penetrability through the Coulomb barrier as well as unwanted background from cosmic rays and beam induced reactions. Therefore several indirect experiments have been conducted to study the compound nucleus of interest ^{26}Mg [16–25]. Most of these experiments have only yielded energy information for states, leaving partial decay widths and spin-parities largely unknown. Discrepancies exist between the deduced energies of the observed levels. Of particular importance as a source of level parameter information were the ^{25}Mg$(n,\gamma)^{26}$Mg experiments by Refs. [24,25] which were later reanalyzed using R-matrix theory by Ref. [26] yielding energies, Γ_n, and Γ_γ parameters for several states over an energy range from the neutron-separation energy up into the energy range accessible by the direct experiments ($E_x > 11.3$ MeV). Also α-transfer reactions, such as those of Refs. [16,17], provide information on α-partial widths.

A recent Nuclear Resonance Fluorescence (NRF) experiment described in Ref. [27], was performed at the

*rdeboer1@nd.edu

High Intensity Gamma-Ray Source (HIγS) at the Triangle Universities Nuclear Laboratory (TUNL). Five states in ^{26}Mg were observed and precise level energy, J^π assignments and γ-branching ratios were reported. In this paper we extend the analysis of Ref. [27] in order to extract the absolute ground-state-transition partial widths for each state.

A brief summary of the relevant NRF technique is presented in Sec. II. Section III describes the analysis. Discussion of the implications of the analysis are covered in Sec. IV. Lastly, Sec. V presents our conclusions.

II. NUCLEAR RESONANCE FLUORESCENCE

Nuclear resonance fluorescence (NRF) represents the photoexcitation of a nucleus with spin J to an excited state with spin J_e followed by its de-excitation to a state i with spin J_i. The theory of NRF has been described in detail (see, e.g., Refs. [28,29]). The analysis applied in the current work follows closely the one presented in Ref. [30] for the case of photon scattering from a thick target.

The number of counts $N_{\rm det}$ in the full-energy peak of the ground-state-transition is given by

$$N_{\rm det} = \Phi(E_R) t_i \epsilon(E_R) W(\theta) A(\Gamma, \Gamma_{\gamma_0}/\Gamma), \tag{1}$$

where $\Phi(E_R)$ is the photon flux, which is assumed to be constant over the Doppler broadened resonance at the energy E_R, t_i is the measuring time corrected for the dead time of the data acquisition, ϵ is the detection efficiency, $W(\theta)$ is the angular distribution of the scattered γ rays relative to the incident beam corrected for the extended detector and target dimensions. The yield $A(\Gamma, \Gamma_{\gamma_0}/\Gamma)$ integrated over the resonance is given by [30]

$$A(\Gamma, \Gamma_{\gamma_0}/\Gamma) = n_t \int_{\rm res} \sigma_{{\rm sc},D}(E) \xi(E)\, dE, \tag{2}$$

where

$$\xi(E) = \frac{1 - e^{-\alpha(E)}}{\alpha(E)} \tag{3}$$

and

$$\alpha(E) = n_t \sigma_{\rm sc,D}(E) \left(\frac{\Gamma}{\Gamma_{\gamma_0}}\right) + C \sum_j \eta_j \sigma_{e,j}(E_R). \tag{4}$$

Here n_t is the number of resonance scatters per unit area in the target, η_j are the number of each different kind of atom per unit area in the target (including the resonance scatters), $\sigma_{e,j}$ are their respective attenuation cross sections which are assumed to be constant over the resonance region, C is a constant that depends only on the geometry of the target and detectors, and $\sigma_{\rm sc,D}(E)$ is the Doppler broadened scattering cross section which depends on the total width of the state Γ and the ground-state-transition branching ratio Γ_{γ_0}/Γ. Note that $\sigma_{\rm sc,D}(E)$ also depends on the Doppler width of the resonance $\Delta = (E/c)(2kT_{\rm eff}/M)^{1/2}$ where k is Boltzmann's constant, M is the mass of ^{26}Mg, and c is the speed of light. The effective temperature, $T_{\rm eff}$, depends on the crystalline structure of the solid and the Debye temperature [28].

Equtaion (3) corrects for nuclear self-absorption and attenuation for a thick target. As the beam passes through the thick target it looses intensity over all energies because of interactions with electrons in the target atoms. The beam also looses additional intensity at the energy of the resonance because of the nuclear interactions of interest. For a *thin* target, where these effects can be neglected ($\alpha \ll 1$), Eq. (2) reduces to

$$A \approx n_t \pi^2 \lambda\!\!\!^{-2} g \left(\frac{\Gamma_{\gamma_0}}{\Gamma}\right)^2 \Gamma, \tag{5}$$

where $g = (2J_e + 1)/(2J + 1)$, $\lambda\!\!\!^{-} = \hbar c/E_R$ and $\hbar$ is Planck's constant divided by 2π.

The next section describes the analysis techniques necessary to extract the total width Γ from Eq. (1) using the spins and branching ratios (Γ_{γ_0}/Γ) for the five resonances reported in Ref. [27].

III. ANALYSIS

The analysis of Ref. [27] obtained precise level energy, J^π assignments, and γ-branching ratios for the five states observed by NRF at the HIγS facility [31]. Here the same data are further analyzed to extract the absolute resonance widths. Linearly polarized and nearly monoenergetic γ rays were made incident on a thick (16.4185 g) isotopically enriched [99.41(6)%] ^{26}MgO sample. The beam had a full width at half maximum of approximately 300 keV requiring four experimental runs at beam energies of 10.8, 11.0, 11.2, and 11.4 MeV in order to cover the energy region of interest. Scattered γ rays were detected using four 60% high purity germanium detectors (HPGe). A detailed description of the experimental setup is given in Ref. [27].

As described in Ref. [27], a GEANT4 Monte Carlo simulation was used to simulate the high purity germanium detectors in order to correct the efficiency and angular distributions for detector and target geometry. Further corrections to the observed full-energy peak intensities from attenuation were performed with the same simulation. As noted in Sec. II the Doppler broadened cross section depends on the Doppler width. For this analysis a room temperature of 293 K and a Debye temperature for MgO powder of 743(8) K [32] was used to determine $T_{\rm eff}$ in the Doppler width formula.

A. Gamma beam flux

The energy distribution of the nearly monoenergetic beam at HIγS was measured by placing a HPGe detector in the beam prior to each of the four production runs. Several copper blocks were placed in the beam to reduce its intensity. The spectrum was corrected for detector response and the relative full-energy peak efficiency as described in Ref. [33] but lacks an absolute normalization.

The integral of the beam-energy distribution was normalized by activating ^{197}Au foils placed in the beam line for the duration of each experimental run utilizing the well known reaction: ^{197}Au$(\gamma,n)^{196}$Au$(EC)^{196}$Pt. Here $t_{1/2}(^{196}{\rm Au}) = 6.1669(6)$ d and the electron capture branching ratio is 93.0(3)% [34]. The intensity of γ-ray transitions from the

355 keV excited state in ^{196}Pt to the ground state was then measured off line in a low-background counting facility.

The observed number of counts in the ^{196}Pt 355 keV photopeak can be found by a slightly modified Eq. (1) from Ref. [35]:

$$N = n_t \epsilon_\gamma f(t) \int_{E_{\rm th}}^{E_{\rm max}} \Phi_\gamma(E)\sigma(E)dE, \qquad (6)$$

where

$$f(t) = \frac{1}{\lambda}(1 - e^{-\lambda t_t})e^{-\lambda t_d}(1 - e^{-\lambda t_m}). \qquad (7)$$

Here n_t is the areal density of ^{197}Au which was approximately 7×10^{20} cm^{-2} for each of the four gold foils, ϵ_γ is the efficiency of the detector for a 355 keV γ ray, λ is the decay constant for ^{196}Au, and t_i(<0.1%), t_d(2%), and t_m(<0.1%) are the irradiation, decay, and measurement times, respectively. $\sigma(E)$ is the ^{197}Au$(\gamma,n)^{196}$Au cross section which is well known (4%) in the energy region [36]. The product of the ^{197}Au(γ,n) cross section and the γ-beam intensity distribution was numerically integrated from the neutron-separation energy $E_{\rm th}$ (8.072 MeV) of ^{197}Au up to the maximum beam energy. Since all other quantities were known experimentally a normalization factor for the absolute flux could be obtained. Values for $\Phi(E_R)$ at the maximum of the beam distribution were between 2×10^4 and 2×10^3 (keV s)$^{-1}$.

IV. DISCUSSION

In the following, previously reported information on the observed states is compared to the measurements here. We discuss briefly the limitations of NRF which effected this study. The impact of the data on astrophysically relevant rate calculations is then addressed.

Because of the low background, several branchings other than the ground-state-transition were observed for each state. With the total widths determined from the analysis above, this allowed for a more confident conversion of the branching ratios from Ref. [27] to the absolute γ widths given it Table I. A summary of the relevant widths measured in previous investigations is given in Table II. Ground-state-transition widths are also given in Weisskopf units and are found to be below the recommended upper limits for γ-ray transition strengths given in Ref. [38].

The state at $E_x = 10647$ keV has been seen in two bremsstrahlung experiments [18,19]. Because of the amount of background in these experiments only the strong ground-state-transition was observed. The ground-state-transition width is lower than that reported by Ref. [19] but agrees well with the more recent value of Ref. [18]. The total width is in agreement with the life time given by Ref. [37]. Five additional branchings were also observed.

The other previously observed state at 11154 keV which is also the only observed level in photon scattering above the neutron-separation energy. This has been seen in the bremsstrahlung experiment of Ref. [18] and the ^{25}Mg$(n,\gamma)^{26}$Mg experiment of Ref. [25]. The later R-matrix analysis of these data by Ref. [26] extracted both the neutron and γ partial widths for this state [$E_n = 62.738(23)$ keV]. In order to properly determine its full width the branching ratio of Ref. [26] was adopted [$\Gamma_\gamma/\Gamma = 4.79(29)/19.2(42) = 0.249(57)$]. The uncertainty in this branching ratio is the most significant uncertainty in the widths since the total width calculation is approximately proportional to its square [see Eq. (5) and Fig. 1]. For convenience of future calculation,

TABLE I. Summary of width calculations for observed ^{26}Mg excited states using the branching ratios of Ref. [27]. Intermediate de-excitation level energies taken from Ref. [37]. γ-partial widths are denoted by their final state energy in keV. Ground-state-transition widths are also given in Weisskopf units (W.u.). Uncertainty for the total width of the 11154 keV state are given by the uncertainties from this work in parentheses followed by the asymmetric uncertainty from the adopted branching ratio of Ref. [26].

Width (eV)	J_f^π	Initial excite state, E_{x_i} (keV), J_i^π				
		10577	10647	10806	10949	11154[a]
		1^-	1^+	1^-	1^-	1^+
Γ_{γ_0}	0^+	0.094(26)	4.12(20)	0.16(4)	0.26(4)	1.91(10)[b]
Γ_{1809}[c]	2^+		0.07(1)	0.56(5)	1.07(5)	0.08(4)[b]
Γ_{2938}[c]	2^+		0.30(2)		0.25(2)	
Γ_{3589}	0^+				0.09(1)	0.31(3)[b]
Γ_{4333}[c]	2^+				0.20(2)	0.21(2)[b]
Γ_{4972}	0^+	0.106(29)	0.08(1)			0.27(5)[b]
Γ_{5292}[c]	2^+		0.08(1)			
Γ_{7100}[c]	2^+		0.06(1)			
Γ_{γ_0} (W.u.)		$1.3(4)\times10^{-4}$	0.163(82)	$2.1(5)\times10^{-4}$	$3.3(5)\times10^{-4}$	0.0656(3)
Γ_γ		0.20(5)	4.70(25)	0.72(18)	1.87(30)	2.78(28)[b]
Γ		0.20(5)	4.70(25)	0.72(18)	1.87(30)	11.2(7)[b]

[a] $\Gamma_\gamma/\Gamma = 0.249$ adopted for this state [26].

[b] Uncertainties are only those of the present experiment. Full uncertainties that include the branching ratio uncertainty of Ref. [26] are given in Table III.

[c] Multipolarity mixing not determined.

TABLE II. Previously measured partial widths (eV) of relevant states in ^{26}Mg.

E_x (keV)	[19]	[37]	[26]	[18]
106 47	$\Gamma_{\gamma_0} = 6.3(7)$	$\Gamma = 6.0(16)$[a]		$\Gamma_{\gamma_0} = 4.65(45)$
111 54			$\Gamma = 19.2(42)$, $\Gamma_\gamma = 4.79(29)$, $\Gamma_n = 14.4(42)$	$\Gamma_{\gamma_0} = 0.252(51)$[b]

[a] [37] reports $\tau_m = 110(30)$ as. Converted to width using $\Gamma = \hbar/\tau_m$.
[b] Assuming $\Gamma_{\gamma_0}/\Gamma = 1$.

Eq. (2) was numerically integrated for several possible values of the branching ratio and the distribution was fit to a power law curve. The distribution shown in Fig. 1 can be used to correct the widths in Table I when a more precise measurement of the branching ratio is obtained. Uncertainties for the partial widths of the 111 54 keV state, including the adopted branching ratio uncertainty from Ref. [26], are given in Table III.

Reference [18] reports a value of $\Gamma_{\gamma_0} = 0.252(51)$ eV for the 111 54 keV state but with the assumption that $\Gamma_{\gamma_0}/\Gamma = 1$. For comparison this value should be corrected by the ground-state-transition γ-branching ratio ($\Gamma_{\gamma_0}/\Gamma_\gamma$) of 0.688(81) and the total γ-branching ratio (Γ_γ/Γ) of 0.249(57). This gives a value of $\Gamma_{\gamma_0} = 1.46(48)$ eV in agreement with the width measured here.

The secondary de-excitation at $E_\gamma = 9136$ keV was also of interest. This γ-ray peak was found to be the transition to the first excited state (109 49 keV $\rightarrow$ 1809 keV) of the 109 49 keV state. The recent bremsstrahlung experiment by Ref. [18] reported a primary transition at 9137.8 keV. It may be possible that Ref. [18] has identified this secondary transition as a primary transition since the ground-state-transition branching ratio of the 109 49 keV state observed here is weak [$\Gamma_{\gamma_0}/\Gamma = 0.138(19)$] and the first excited state branching ratio is dominant [$\Gamma_{1809}/\Gamma = 0.572(29)$]. If there were two different γ-ray peaks, they would only be separated by 2 keV making them unresolvable by Ref. [18]. The measurement from Ref. [18] reports the 9137.8 keV state as ($0 \rightarrow 1 \rightarrow 0$) transition while the observed secondary transition of this experiment at 9136 keV was ($0 \rightarrow 1 \rightarrow 2$). In Ref. [18] intensities were measured at 90° and 127° where the relative intensities of the angular distribution should be 0.73 and 1 for ($0 \rightarrow 1 \rightarrow 0$) and ($0 \rightarrow 1 \rightarrow 2$) transitions respectively making differences in intensity difficult to distinguish. The width observed here [1.07(5) eV] is substantially different from that given in Ref. [18] [$\Gamma = 0.131(32)$ eV]. This should be corrected by the branching ratio observed here [$\Gamma_{1808}/\Gamma = 0.572(29)$], which would give value of $\Gamma = 0.229(57)$ eV, but a significant difference is still present.

TABLE III. The uncertainty from the present experiment is combined with the uncertainty from the neutron branching ratio of Ref. [26] to give the total uncertainty on the widths of the 111 54 keV state.

Decay channel	Total uncertainty (eV)
Γ_{γ_0}	$+1.31, -0.65$
Γ_{1809}	$+0.06, -0.03$
Γ_{3589}	$+0.21, -0.11$
Γ_{4333}	$+0.14, -0.07$
Γ_{4972}	$+0.19, -0.09$
Γ_γ	$+1.93, -0.95$
Γ	$+7.7, \quad -3.8$

Several states are known to exist in the excitation energy region (see Sec. I) that were not observed. Part of the reason for this is the limitations inherent to NRF. The first limitation is that the $J = 1$ spin of the photon makes it difficult to excite excitation levels of $J > 1$ in spin $J = 0$ nuclei. The second limitation is that the excited state must be populated through the ground state γ transition. If the state has a small ground state γ-branching ratio it may not be observed. This limitation becomes even more pronounced once the neutron channel opens. Special effort was made to excite the lowest energy state at $E_x \approx 11.319$ keV ($E_\alpha \approx 830$ keV), observed in past ^{22}Ne(α,n)^{25}Mg and ^{22}Ne(α,γ)^{26}Mg reaction experiments, in order to investigate the possibility of a doublet in this region [26], but no state was observed. This is most likely explained by the branching ratios reported for this state by Ref. [13].

The ^{22}Ne + α reactions are limited to states of natural parity by angular momentum selection rules. Three of the observed states are $J = 1^-$ with two above the α-separation energy. As pointed out in Ref. [27] the one state observed above the neutron-separation energy at 111 54 keV is $J = 1^+$. This state has long been suspected of being natural parity [20] and several experiments have attempted to observe this state by ^{22}Ne(α,n)^{25}Mg [11,12,14,16] with only upper limits reported. The two states at $E_x = 10805.7(7)$ and

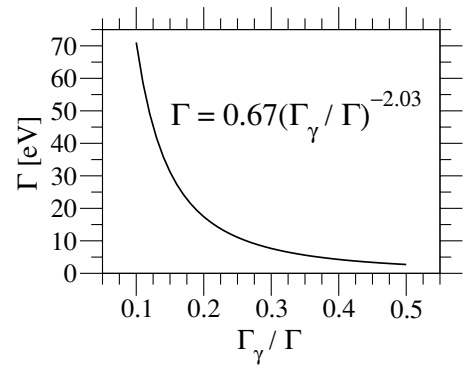

FIG. 1. The total width in eV as a function of the γ-branching ratio. A power law [$\Gamma = A(\Gamma_\gamma/\Gamma)^{-B}$] fit was found to reproduce the distribution well over the entire branching ratio parameter space. A χ^2 fit, using only the uncertainties associated with this experiment, was done to determine the uncertainty in the fit parameters. For two fit parameters $\Delta\chi^2 = \chi^2_{\min} + 2.41$ for a 70% confidence level [39]. The fit parameter values were $A = 0.67(12)$ and $B = 2.03(27)$.

10949.1(8) keV ($E_{\mathrm{c.m.}} = 191$ and 334 keV) will contribute to the ^{22}Ne$(\alpha,\gamma)^{26}$Mg reaction rate.

A rate calculation requires the additional knowledge of the α-widths of these states. The energy region has been investigated with the α-transfer reaction ^{22}Ne(^{6}Li, d)^{26}Mg by Refs. [16,17] and spectroscopic factors S_α were determined for two resonances whose energies closely match those observed here. Reference [16] measured the angular distribution for a state at $E_x = 10.949(25)$ MeV which was later resolved into two states at $E_x = 10.808(20)$ and 10.953(25) MeV by Ref. [17]. A DWBA analysis was performed by both Refs. [16,17] to determine the most likely J^π of the states. The assumption is that the two states observed by Ref. [17] at 10.808(20) ($J^\pi = 0^+ - 4^+$) and 10.953(25) MeV ($J^\pi = 5^- - 7^-$) are those observed here at 10.8057(7) ($J^\pi = 1^-$) and 10.9491(8) MeV ($J^\pi = 1^-$) as suggested in Ref. [27]. For this reason a DWBA calculation was performed using the code DWUCK4 [40] in order to recalculate the spectroscopic factors with the new spin assignment from Ref. [27]. Potential parameters were the same as those given in Ref. [16]. It was found that the DWBA calculation for an angular distribution of $J^\pi = 1^-$ for both states does not compared well to the data of Ref. [16]. Because of the limited energy resolution of the α-transfer experiments, the poor agreement with angular distribution calculations, and the high level density of ^{26}Mg in this energy region, it is likely that one or both of the states observed in the α-transfer experiments are not the same as those observed here.

V. SUMMARY

Five states were reported by Ref. [27] in ^{26}Mg and precise level energy, J^π assignments and γ-branching ratios were found. Due to the thick target, corrections for nuclear self absorption were made using Eq. (1) and attenuation using GEANT4 in order to obtain absolute ground-state-transition partial widths. Secondary transition γ widths were calculated using the branching ratios of Ref. [27]. The high sensitivity to secondary de-excitation make the calculation of the total widths quite reliable. Three states at 10573 keV, 10806 keV, and 10949 keV have partial width information presented for the first time. For the other two states, the partial widths of the state at $E_x = 10647$ keV are in good agreement with those of previous works. The state at $E_x = 11154$ keV was found to have partial widths about half as strong as those given in Refs. [25,26] but was found to agree within the uncertainty of the neutron branching ratio. The two natural parity states identified at 10806 and 10949 keV can contribute to the ^{22}Ne$(\alpha,\gamma)^{26}$Mg reaction rate.

Without measured spectroscopic factors a more accurate calculation of the contribution to the (α,γ) rate by the two states is not achievable at this time. As a main source of neutrons for the s-process, the uncertainty in the partial widths of ^{26}Mg natural parity states has a significant effect on simulations of heavy element production. The critical excitation energy range in the compound nucleus ^{26}Mg is 10.9 MeV $< E_x <$ 11.5 MeV overlapping the neutron-separation energy at 11.1 MeV. With the high level density many states could contribute significantly to the rate. A detailed knowledge of the states in this energy region is still incomplete prompting further studies.

ACKNOWLEDGMENTS

This work was funded by the National Science Foundation through Grant No. Phys-0758100, and the Joint Institute for Nuclear Astrophysics Grant No. Phys-0822648.

[1] U. Ratzel, C. Arlandini, F. Käppeler, A. Couture, M. Wiescher, R. Reifarth, R. Gallino, A. Mengoni, and C. Travaglio, Phys. Rev. C **70**, 065803 (2004).
[2] I. Iben Jr., Astrophys. J. **196**, 525 (1975).
[3] F. Käppeler, H. Beer, and K. Wisshak, Rep. Prog. Phys. **52**, 945 (1989).
[4] D. Hollowell and I. J. Iben, Astrophys. J. Lett. **333**, L25 (1988).
[5] M. Pignatari, R. Gallino, F. Käppeler, and M. Wiescher, Nucl. Phys. A **758**, 541 (2005).
[6] L.-S. The, M. F. E. Eid, and B. S. Meyer, Astrophys. J. **655**, 1058 (2007).
[7] A. I. Karakas, M. A. Lugaro, M. Wiescher, J. Görres, and C. Ugalde, Astrophys. J. **643**, 471 (2006).
[8] A. H. Wapstra, G. Audi, and C. Thibault, Nucl. Phys. A **729**, 129 (2003); the 2003 NUBASE and Atomic Mass Evaluations [http://www.sciencedirect.com/science/article/B6TVB-4B4VNB4-3/2/cce5348f4cd31847bbbde9b5b16cddc8].
[9] D. Ashery, Nucl. Phys. A **136**, 481 (1969).
[10] F. X. Haas and J. K. Bair, Phys. Rev. C **7**, 2432 (1973).
[11] H. Drotleff, A. Denker, J. Hammer, H. Knee, S. Küchler, D. Streit, C. Rolfs, and H. Trautvetter, Z. Phys. A **338**, 367 (1991).
[12] V. Harms, K.-L. Kratz, and M. Wiescher, Phys. Rev. C **43**, 2849 (1991).
[13] K. Wolke, V. Harms, H. Becker, J. Hammer, K. Kratz, C. Rolfs, U. Schroder, H. Trautvetter, M. Wiescher, and A. Wohr, Z. Phys. A **334**, 491 (1989).
[14] M. Jaeger, R. Kunz, A. Mayer, J. Hammer, G. Staudt, K. Kratz, and B. Pfeiffer, Phys. Rev. Lett. **87**, 202501 (2001).
[15] E. Kuhlmann, E. Ventura, J. R. Calarco, D. G. Mavis, and S. S. Hanna, Phys. Rev. C **11**, 1525 (1975).
[16] U. Giesen, C. P. Browne, J. Görres, S. Graff, C. Iliadis, H. P. Trautvetter, M. Wiescher, W. Harms, K. L. Kratz, B. Pfeiffer *et al.*, Nucl. Phys. A **561**, 95 (1993).
[17] C. Ugalde, A. E. Champagne, S. Daigle, C. Iliadis, R. Longland, J. R. Newton, E. Osenbaugh-Stewart, J. A. Clark, C. Deibel, A. Parikh *et al.*, Phys. Rev. C **76**, 025802 (2007).
[18] R. Schwengner, A. Wagner, Y. Fujita, G. Rusev, M. Erhard, D. D. Frenne, E. Grosse, A. R. Junghans, K. Kosev, and K. D. Schilling, Phys. Rev. C **79**, 037303 (2009).
[19] U. E. P. Berg, K. Ackermann, K. Bangert, C. Blsing, W. Naatz, R. Stock, K. Wienhard, M. K. Brussel, T. E. Chapuran, and B. H. Wildenthal, Phys. Lett. B **140**, 191 (1984).
[20] B. L. Berman, R. L. Van Hemert, and C. D. Bowman, Phys. Rev. Lett. **23**, 386 (1969).
[21] S. C. Fultz, R. A. Alvarez, B. L. Berman, M. A. Kelly, D. R. Lasher, T. W. Phillips, and J. McElhinney, Phys. Rev. C **4**, 149 (1971).

[22] C. Moss, Nucl. Phys. A **269**, 429 (1976).
[23] G. M. Crawley, C. Djalali, N. Marty, M. Morlet, A. Willis, N. Anantaraman, B. A. Brown, and A. Galonsky, Phys. Rev. C **39**, 311 (1989).
[24] T. A. Walkiewicz, S. Raman, E. T. Jurney, J. W. Starner, and J. E. Lynn, Phys. Rev. C **45**, 1597 (1992).
[25] H. Weigmann, R. L. Macklin, and J. A. Harvey, Phys. Rev. C **14**, 1328 (1976).
[26] P. E. Koehler, Phys. Rev. C **66**, 055805 (2002).
[27] R. Longland, C. Iliadis, G. Rusev, A. P. Tonchev, R. J. deBoer, J. Görres, and M. Wiescher, Phys. Rev. C **80**, 055803 (2009).
[28] F. R. Metzger, Prog. Nucl. Phys. **7**, 54 (1959).
[29] W. Hamilton, *The Electromagnetic Interaction in Nuclear Spectroscopy* (North-Holland Publishing Company/American Elsevier Publishing Company, Amsterdam/New York, 1975), Chap. 8, p. 283: Nuclear Resonance Fluorescence by S. J. Skorka.
[30] T. Chapuran, R. Vodhanel, and M. K. Brussel, Phys. Rev. C **22**, 1420 (1980).
[31] H. R. Weller, M. W. Ahmed, H. Gao, W. Tornow, Y. K. Wu, M. Gai, and R. Miskimen, Prog. Part. Nucl. Phys. **62**, 257 (2009).
[32] M. M. Beg, Acta Crystallogr. Sect. A **32**, 154 (1976).
[33] G. Rusev, A. P. Tonchev, R. Schwengner, C. Sun, W. Tornow, and Y. K. Wu, Phys. Rev. C **79**, 047601 (2009).
[34] H. Xiaolong, Nucl. Data Sheets **108**, 1093 (2007).
[35] A. P. Tonchev, C. T. Angell, M. Boswell, A. S. Crowell, B. Fallin, S. Hammond, C. R. Howell, A. Hutcheson, H. J. Karwowski, J. H. Kelley *et al.*, Phys. Rev. C **77**, 054610 (2008).
[36] V. Varlamov, N. Peskov, D. Rudenko, and M. Stepanov, Vop. At. Nauki i Tekhn. Ser. Yadernye Konstanty **1**, 48 (2003), eXFOR # M0635.112.
[37] P. M. Endt, Nucl. Phys. A **633**, 1 (1998).
[38] P. M. Endt, At. Data Nucl. Data Tables **55**, 171 (1993) [http://www.sciencedirect.com/science/article/B6WBB-45R7DJT-H/2/9cdd53bc9291a3d1ec9a09b46e2724f3].
[39] F. James, MINUIT: Function Minimization and Error Analysis Reference Manual, CERN, CERN Geneva, Switzerland, version 94.1 ed. (2000), CERN Program Library Long Writeup D506.
[40] P. Kunz, program DWUCK4, extended version by J. Comfort (unpublished 1983).